Korean J. Chem. Eng., 32(9), 1798-1803 (2015)
DOI: 10.1007/s11814-014-0387-6

pISSN: 0256-1115
eISSN: 1975-7220

A two-dimensional analytical model of laminar flame in lycopodium dust particles

Alireza Rahbari*,†, Ashkan Shakibi, and Mehdi Bidabadi****

*Department of Mechanical Engineering, Shahid Rajaee Teacher Training University (SRTTU), Tehran, Iran
**Department of Mechanical Engineering, Iran University of Science and Technology,
Combustion Research Laboratory, Narmak, Tehran, Iran
(*Received 15 May 2014 • accepted 26 December 2014*)

Abstract−A two-dimensional analytical model is presented to determine the flame speed and temperature distribution of micro-sized lycopodium dust particles. This model is based on the assumptions that the particle burning rate in the flame front is controlled by the process of oxygen diffusion and the flame structure consists of preheat, reaction and post flame zones. In the first step, the energy conservation equations for fuel-lean condition are expressed in two-dimensions, and then these differential equations are solved using the required boundary condition and matching the temperature and heat flux at the interfacial boundaries. Consequently, the obtained flame temperature and flame speed distributions in terms of different particle diameters and equivalence ratio for lean mixture are compared with the corresponding experimental data for lycopodium dust particles. Consequently, it is shown that this two-dimensional model demonstrates better agreement with the experimental results compared to the previous models.

Keywords: Lycopodium Dust Particles, Two-dimensional Analytical Model, Laminar Flame Speed, Flame Temperature Distribution

INTRODUCTION

Research on different characteristics and aspects of combustible particles is ongoing and many experimental and theoretical studies on the properties of flame propagation in dust clouds have been conducted [1-4]. Nevertheless, knowledge on fundamental phenomenon of dust flame propagation is still imprecise and insufficient to explain the mechanism of flame propagation in dust clouds.

Ignition and combustion of particle dust clouds have been actively studied over the last five decades with a large number of experimental data accumulated [5-7].

Goroshin et al. [8] defined the flame thickness for the reaction zone proportional to the burning velocity and combustion time for aluminum dust particles. Since aluminum dust particles do not vaporize during combustion, the vaporization term was not considered in the governing equations, while this term must be taken into account for the lycopodium dust particles.

Han et al. [9,10] conducted an experimental study to elucidate the structure of flame propagation through lycopodium dust clouds in a vertical duct. The maximum upward propagating velocity was 0.50 m/s at a dust concentration of 170 g/m^3. Despite the employment of nearly equal sized particles and their good dispersability and flowability, the reaction zone in lycopodium particles cloud showed a double flame structure, consisting of enveloped diffusion flames (spot flame) of individual particles and diffusion flames (independent flame) surrounding some particles. Proust [11,12] measured the laminar burning velocities and maximum flame temperatures for combustible dust-air mixtures such as starch dust-air mixtures, lycopodium-air mixtures and sulphur flour-air mixtures.

In the previous study, Bidabadi and Rahbari [13] analytically investigated the flame propagation through lycopodium dust particles, containing uniformly distributed volatile fuel particle and explored the flame structure mechanism and the effect of temperature difference between gas and particle on the combustion characteristics. Bidabadi and Rahbari [14] presented a novel analytical model for predicting the heat loss and Lewis number effects on the combustion of Lycopodium particles. In a recent study [15], the aspects of flame propagation and the structure of combustion zone were analytically investigated to clarify the mechanisms of flame propagation through organic dust cloud. In this research, the effects of different Lewis and Damköhler numbers and the initiation of particles vaporization on the combustion phenomenon of the organic dust particles were completely specified.

In the previous research, Bidabadi et al. [16] presented a one-dimensional model for predicting the flame temperature through lycopodium dust particles. In this research, the radiation and heat loss effects on the premixed flame propagation were considered. Furthermore, in [17], a mathematical model was proposed to determine the thermophoresis effect on volatile particle concentration in micro-organic dust flame.

Gao et al. [18] studied the effects of particle size distributions on flame propagation mechanism during dust explosions. A simple mathematical model was developed to determine the critical particle size to illustrate the flame propagation mechanisms in dust explosions.

Jadidi and Bidabadi [19] analytically investigated the flame propagation through aluminum dust particles, developing two-dimensional condition for lean and rich mixtures and showed that solving

†To whom correspondence should be addressed.
E-mail: ar.rahbari@gmail.com

equations in two-dimensional models leads to higher agreements between the theoretical and experimental results.

In this study, a new analytical model for the combustion of lycopodium dust particles is developed based on a model presented by Goroshin et al. [8,20]. To achieve this objective, a similar approach for the aluminum dust combustion is used considering the point that the lycopodium dust particles vaporize during the combustion phenomenon, and therefore a vaporization term must be added into the governing equations. In addition, based on the achieved findings [19], a two-dimensional model declares a better adjustment with the experimental data. Hence, the main emphasis of this study is made on proposing a comprehensive two-dimensional model in comparison with the previous researches [13-16].

MATHEMATICAL MODELING

The analytical model described below is based on a two-dimensional approximation of the flame with conductive heat losses. The major assumptions and approximations are: (1) the dust cloud consists of a mixture of gaseous oxidizer and uniformly distributed, equal-sized lycopodium particles, (2) the gravitational effects are neglected, (3) the particle velocity is equal to the gas velocity in the laminar, steady and uniform flow, and (4) the Biot number for the particle is very small, implying that the temperature of a particle is uniform.

1. Dust Flame in a Lean Mixture

In this research, after following [8,16,20], we assumed that the flame structure consists of three zones: preheat, flame, and post flame zones, as illustrated in Fig. 1.

The first zone is the preheat zone (x<0), where the temperature of particles is lower than the ignition temperature, and therefore the rate of reaction is negligible. In this zone, the gas is heated by conduction from the flame zone and particles are heated by the surrounding gas until their temperature reaches its ignition point. The difference in temperature between the dust particles and the gas progressively increases due to inertia in the heat exchange. The second zone is the flame zone (0<x<δ), where particles are ignited and totally consumed. The flame thickness is much less than the total combustion distance**.** The last zone is the post flame zone (x> δ), where the gas temperature gradually returns to the initial value T_u due to heat loss in this zone.

Based on the previous researches [8,16,20], it is assumed that the particle temperature at the moment of ignition (x=0), is close to the auto ignition temperature of a single particle T_{si} (the ignition temperature in a gas media of constant temperature) and can be found from the equation describing inert particle heating in the preheat zone:

$$v_u m_s c_s \frac{dT_s}{dx} = \frac{\lambda_s}{r}(4\pi r^2)(T_s - T) \tag{1}$$

The one-dimensional gas phase governing equations for energy conservation can be written as:

$$\rho V C \frac{dT}{dx} = \lambda \nabla^2 T - w_v Q_v + w_f Q \tag{2}$$

where ρ, V and T are gas density, velocity, and temperature, respectively. C stands for the specific heat of gas at constant pressure, c_s for the specific heat of particle, w_f for the reaction rate characterizing consumption of fuel, w_v for the vaporization rate, Q for the combustion heat release, Q_v for the heat associated with vaporization of the particle, r for the particle radius and T_s for the particle temperature. By solving the energy equation in each zone and matching the temperature and heat flux at the interfacial boundaries, an algebraic equation for the flame speed in a fuel-lean mixture can be found.

Following the previous one-dimensional research [8,16,20] for obtaining flame speed and temperature distribution, in the present study, a two-dimensional analytical model of laminar flame in lycopodium dust particles is represented. As mentioned, the flame structure is divided into the three preheat, flame, and post flame zones. By solving the partial differential equations of energy in the two-dimensional condition and using the separation of variables method in all the three zones and satisfying the boundary conditions, an algebraic equation for the flame speed as a function of equivalence ratio and gas phase temperature distribution are determined. The experimental data shows the quenching plate temperature does not exceed and is almost equal to that of the initial or the unburned mixture temperature. Therefore, this temperature is assumed to be constant ($T=T_u$). Moreover, the thermal conductivity of gas, λ, which usually varies with temperature, is taken to be constant for the sake of simplicity.

With these assumptions, the gas phase governing heat diffusivity equation and the boundary conditions for the problem can be obtained:

Preheat zone

$$\rho V C \frac{dT_1}{dx} = \lambda\left(\frac{\partial^2 T_1}{\partial x^2} + \frac{\partial^2 T_1}{\partial y^2}\right) - w_v Q_v \tag{3}$$

Flame zone

$$\rho V C \frac{dT_2}{dx} = \lambda\left(\frac{\partial^2 T_2}{\partial x^2} + \frac{\partial^2 T_2}{\partial y^2}\right) + w_f Q \tag{4}$$

Post flame zone

$$\rho V C \frac{dT_3}{dx} = \lambda\left(\frac{\partial^2 T_3}{\partial x^2} + \frac{\partial^2 T_3}{\partial y^2}\right) \tag{5}$$

Considering new parameter $\theta=T-T_u$, new governing equations are as follows:

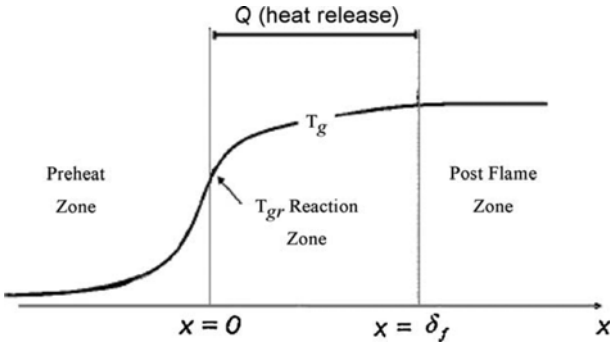

Fig. 1. The flame structure of lycopodium dust particles.

Preheat zone

$$\frac{\partial^2\theta_1}{\partial x^2}+\frac{\partial^2\theta_1}{\partial y^2}-2S\frac{d\theta_1}{dy}-k\theta=kT_u \tag{6}$$

Flame zone

$$\frac{\partial^2\theta_2}{\partial x^2}+\frac{\partial^2\theta_2}{\partial y^2}-2S\frac{d\theta_2}{dy}=-R\phi \tag{7}$$

Post flame zone

$$\frac{\partial^2\theta_3}{\partial x^2}+\frac{\partial^2\theta_3}{\partial y^2}-2S\frac{d\theta_3}{dy}=0 \tag{8}$$

The parameters, k, ϕ, S, R in the above equations are defined as

$$\begin{aligned} &w_vQ_v/\lambda=An_s4\pi r^2TQ_v/\lambda=kT \qquad k=An_s4\pi r^2TQ_v/\lambda\\ &w_fQ/\lambda=BvQ/\lambda\delta=B_{st}\phi vQ/\lambda\delta=R\phi \qquad \phi=B/B_{st}\\ &S=\rho vC_p/2\lambda \qquad R=B_{st}vQ/\lambda\delta \end{aligned} \tag{9}$$

Boundary conditions

$$\begin{aligned} &\frac{\partial\theta_1}{\partial x}(-\infty,y)=0 \qquad \frac{\partial\theta_3}{\partial x}(+\infty,y)=0 \qquad \theta_1(x,0)=\theta_1(x,d)=0\\ &\theta_1(0,y)=\theta_2(0,y) \quad \frac{\partial\theta_1}{\partial x}(0,y)=\frac{\partial\theta_2}{\partial x}(0,y) \quad \theta_2(x,0)=\theta_2(x,d)=0\\ &\theta_2(0,y)=\theta_3(0,y) \quad \frac{\partial\theta_2}{\partial x}(0,y)=\frac{\partial\theta_3}{\partial x}(0,y) \quad \theta_3(x,0)=\theta_3(x,d)=0 \end{aligned} \tag{10}$$

By solving the above equations the following solutions are obtained

$$\theta_1(x,y)=\sum_{n=1}^{\infty}a_n e^{(s+\sqrt{s^2+\mu_n^2+k})x}\sin(\mu_n y) + \left[\left(\frac{e^{\sqrt{k}d}-1}{e^{2\sqrt{k}d}-1}\right)e^{\sqrt{k}y}+\left(\frac{e^{2\sqrt{k}d}-e^{\sqrt{k}d}}{e^{2\sqrt{k}d}-1}\right)e^{-\sqrt{k}y}-1\right]T_u \tag{11}$$

$$\theta_2(x,y)=\sum_{n=1}^{\infty}b_n\left(-\frac{s-\sqrt{s^2+\mu_n^2}}{s+\sqrt{s^2+\mu_n^2}}e^{(-2\sqrt{s^2+\mu_n^2})\delta}e^{(s+\sqrt{s^2+\mu_n^2})x} + e^{(s-\sqrt{s^2+\mu_n^2})x}\right)\sin(\mu_n y)+\sum_{n=1}^{\infty}c_n\left(-\frac{s-\sqrt{s^2+\mu_n^2}}{s+\sqrt{s^2+\mu_n^2}}e^{(s+\sqrt{s^2+\mu_n^2})x} + e^{(s-\sqrt{s^2+\mu_n^2})x}\right)\sin(\mu_n y)+0.5R\phi y(d-y) \tag{12}$$

$$\theta_3(x,y)=\sum_{n=1}^{\infty}d_n e^{(s-\sqrt{s^2+\mu_n^2})x}\sin(\mu_n y) \tag{13}$$

where

$$\mu_n=\frac{n\pi}{d} \qquad n=1,2,3,\ldots \tag{14}$$

The first term at the right hand of Eqs. (11)-(12) can be expanded as follows:

$$\left[\left(\frac{e^{\sqrt{k}d}-1}{e^{2\sqrt{k}d}-1}\right)e^{\sqrt{k}y}+\left(\frac{e^{2\sqrt{k}d}-e^{\sqrt{k}d}}{e^{2\sqrt{k}d}-1}\right)e^{-\sqrt{k}y}-1\right]T_u=\sum_{n=1}^{\infty}E_n\sin(\mu_n y) \tag{15}$$

$$0.5R\phi y(d-y)=\sum_{n=1}^{\infty}F_n\sin(\mu_n y) \tag{16}$$

where

$$E_n=\frac{-2kd^2T_u}{kd^2n\pi+(n\pi)^3}(1-\cos(n\pi)) \tag{17}$$

$$F_n=\frac{-2R\phi d^2}{(n\pi)^3}(1-\cos(n\pi)) \tag{18}$$

The boundary conditions described in Eq. (10) are used to obtain coefficients a_n, b_n, c_n and d_n as below:

$$\begin{aligned} a_n&=b_n\frac{s-\sqrt{s^2+\mu_n^2}}{s+\sqrt{s^2+\mu_n^2+k}}(1-e^{(-2\sqrt{s^2+\mu_n^2})\delta})\\ b_n&=\frac{(E_n-F_n)e^{(s+\sqrt{s^2+\mu_n^2})\delta}+F_n}{\gamma e^{(s+\sqrt{s^2+\mu_n^2})\delta}-\beta e^{(s-\sqrt{s^2+\mu_n^2})\delta}}\\ c_n&=\frac{\beta(E_n-F_n)e^{(s-\sqrt{s^2+\mu_n^2})\delta}-\gamma F_n}{-\beta\gamma e^{(s+\sqrt{s^2+\mu_n^2})\delta}+\beta^2 e^{(s-\sqrt{s^2+\mu_n^2})\delta}}\\ d_n&=c_n(1+e^{2\sqrt{s^2+\mu_n^2}\delta}) \end{aligned} \tag{19}$$

where

$$\begin{aligned} \beta&=1-\frac{s-\sqrt{s^2+\mu_n^2}}{s+\sqrt{s^2+\mu_n^2}}\\ \gamma&=\left(\frac{s-\sqrt{s^2+\mu_n^2}}{s+\sqrt{s^2+\mu_n^2+k}}-\frac{s-\sqrt{s^2+\mu_n^2}}{s+\sqrt{s^2+\mu_n^2}}\right)e^{(-2\sqrt{s^2+\mu_n^2})\delta}-\frac{s-\sqrt{s^2+\mu_n^2}}{s+\sqrt{s^2+\mu_n^2+k}}+1 \end{aligned} \tag{20}$$

The heat transfer between each particle and surrounding gas is given by:

$$q=hA(T-T_s)=\frac{Nu\cdot\lambda}{2r}4\pi r^2(T-T_s)=4\pi r\lambda(T-T_s) \tag{21}$$

where the Nusselt number is considered equal to 2.

The energy conservation equation for the solid phase is

$$\frac{\partial\theta_s}{\partial x}=\xi(\theta_1-\theta_s) \tag{22}$$

where

$$\xi=\frac{3\lambda}{r^2\rho CV} \qquad \theta_s=(T_s-T_u) \tag{23}$$

Boundary condition for Eq. (22)

$$x\to-\infty\Rightarrow\theta_s=0 \tag{24}$$

By solving Eq. (22) and using the boundary condition (24), the solid phase temperature of the fuel-lean mixture is obtained as:

$$\theta_s(x,y)=\sum_{n=1}^{\infty}\left(\frac{\xi a_n}{s+\sqrt{s^2+\mu_n^2+k}+\xi}e^{(s+\sqrt{s^2+\mu_n^2+k})x}+E_n\right)\sin(\mu_n y) \tag{25}$$

Also, since the particle temperature at x=0 equals the ignition temperature, T_{si}, we have

$$\theta_{si}=\sum_{n=1}^{\infty}\left(\frac{\xi a_n}{s+\sqrt{s^2+\mu_n^2+k}+\xi}+E_n\right)\sin(\mu_n y) \tag{26}$$

where $\theta_{si}=T_{si}-T_u$

θ_{si} is expanded as follows

$$\theta_{si}=\sum_{n=1}^{\infty}\theta_n \mathrm{Sin}(\mu_n y) \tag{27}$$

where (utilizing the orthogonality of functions):

$$\theta_n=\frac{-2\theta_{st}}{n\pi}(1-\mathrm{Cos}(n\pi)) \tag{28}$$

Comparing Eqs. (26) and (27) leads to the following equation for θ_n:

$$\theta_n=\frac{\xi a_n}{s+\sqrt{s^2+\mu_n^2}+k+\xi}+E_n \tag{29}$$

Using Eqs. (28) and (29) and simplifying them, the key equation of flame speed as a function of equivalence ratio is obtained for the two-dimensional condition, which is accurate for each quantity of n as:

$$\begin{aligned}\phi=&e^{(s+\sqrt{s^2+\mu_n^2})\delta}(k\xi d^2 n^2\pi^2 ST_u(1-e^{2(\sqrt{s^2+\mu_n^2})\delta})\\&+(s+\sqrt{s^2+\mu_n^2}+k+\xi)(kd^2T_u+\theta_{si}(kd^2+n^2\pi^2))\\&\times(d^2S(1+e^{2(\sqrt{s^2+\mu_n^2})\delta})(s+\sqrt{s^2+\mu_n^2})(s+\sqrt{s^2+\mu_n^2}+k)\\&+n^2\pi^2(S(1+e^{2(s^2+\mu_n^2)\delta})+2\sqrt{s^2+\mu_n^2}+k)))\\&/(R\xi d^2(e^{2\sqrt{s^2+\mu_n^2}\delta}-1)(kd^2+n^2\pi^2)(e^{(s+\sqrt{s^2+\mu_n^2})\delta}(s+\sqrt{s^2+\mu_n^2})))\end{aligned} \tag{30}$$

The following initial parameters are used in this research to determine the flame speed and gas phase temperature distribution [13-16]:

$\lambda=3.5\times10^{-4}$ Cal/cm·s·K	$A=3.4\times10^{-6}$ gr/cm^2·K	$\rho=6.5\times10^{-3}$ gr/cm^3
C=0.33 Cal/gr·K	$B_{st}=125$ gr/m^3	$T_{si}=1500$ K
$T_u=300$ K	Q=12400 kj/kg	$Q_v=124$ kj/kg
$n_s=4500$ 1/cm^3		

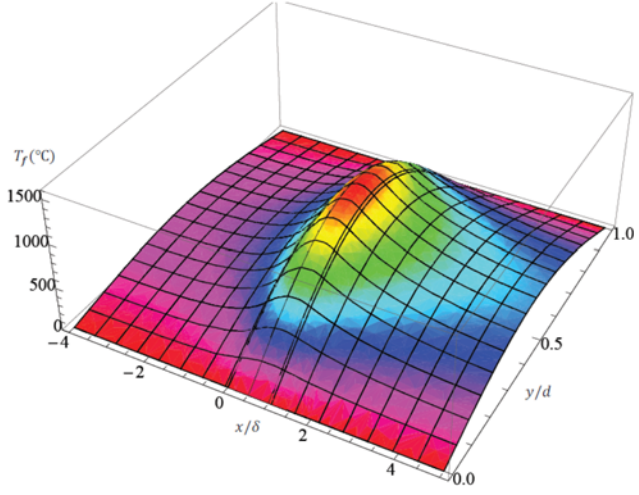

Fig. 2. Temperature profile of lycopodium dust particles in a two-dimensional model.

RESULTS AND DISCUSSION

Fig. 2 shows the gas temperature distribution in preheat, flame, and post flame zones for the fuel-lean mixture, which are obtained from Eqs. (11), (12), and (13) in the two-dimensional model. This figure displays efficiently the temperature changes in all three zones. The temperature in the middle of the channel is in accordance with the temperature curves of the one-dimensional models.

In the preheat zone, gas is heated by conduction from the flame zone. In the flame zone, despite the smallness of the zone relative to the other zones, gas has an almost constant temperature. In the post flame zone, the temperature decreases finally down to the initial temperature. With the assumption that the particles are uniformly distributed, temperature profiles are obtained in a symmetrical relation to the channel center.

Fig. 3 depicts the flame temperature variation as a function of dust concentration. As seen, the obtained result from the present model is compared with the theoretical model Han et al. [9] and Proust (reported by Han et al. [9]) and the experimental data [9].

The experimental flame temperature varies from 1,000 to 1,200 °C, while Han et al. [9] model forecasts the flame temperature lower than the experimental data, in the range of 900 to 1,050 °C. Although the Proust (reported by Han et al. [9]) model prediction agrees with the experimental result [9] at lower dust concentration, its anticipation is not reasonable at higher dust concentration. But in the

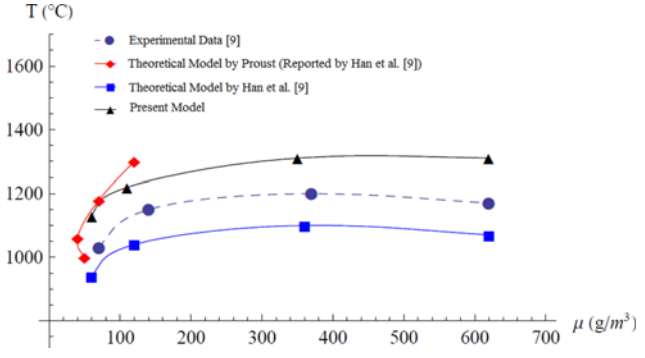

Fig. 3. The flame temperature as a function of dust concentration in lycopodium particles.

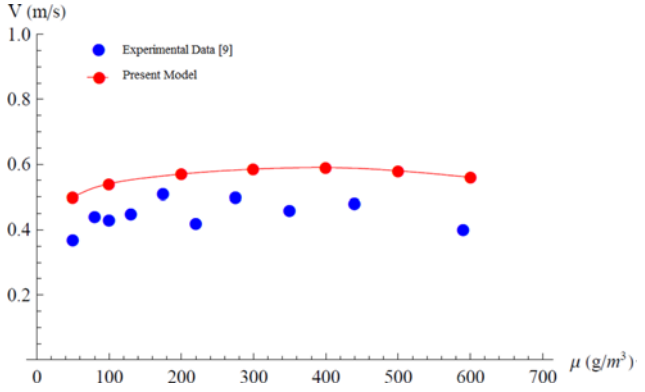

Fig. 4. Flame speed as a function of dust concentration in lycopodium particles.

present model, the measured flame temperature, changing from 1,100 to 1,300, is fairly comparable with the corresponding experimental data and, moreover, the trend of the flame temperature complies with the experimental behavior.

Fig. 4 shows the flame speed distribution in terms of concentration for fuel lean mixture both for the present model and the experimental data [9]. In this figure particle diameter is d_p=32 μm and there is a good agreement between the obtained and experimental flame speed. This is a finding which indicates the importance of considering a two-dimensional model. As seen, the flame speed of this model is higher than the experimental result. This discrepancy is justifiable by the heat loss and radiation effects which are not considered in this research.

Fig. 5 indicates the flame speed as a function of dust concentration for different particle diameters. As observed, the flame speed trend is the same for different particle diameters when the dust concentration increases. From this figure, it can be concluded that the flame speed goes up and down when the dust concentration increases and higher flame speed is achieved for the lower particle diameter.

Fig. 6 indicates the calculated two-dimensional laminar flame speed as a function of equivalence ratio for lycopodium-air mixtures. The flame speed increases with decreasing particle size. Based on the assumptions of this study, flame speed increases gradually with the increase of equivalence ratio.

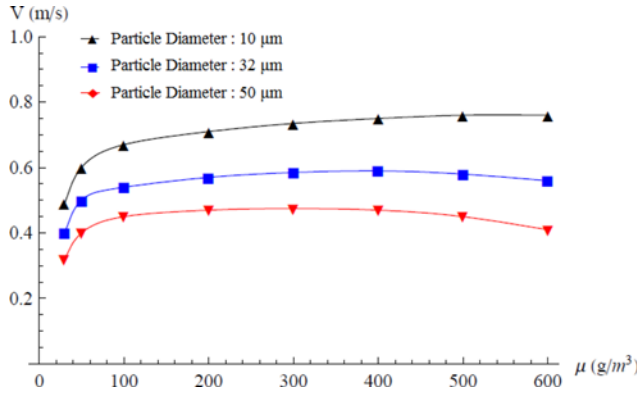

Fig. 5. Flame speed as a function of dust concentration in lycopodium particles for different particle diameters.

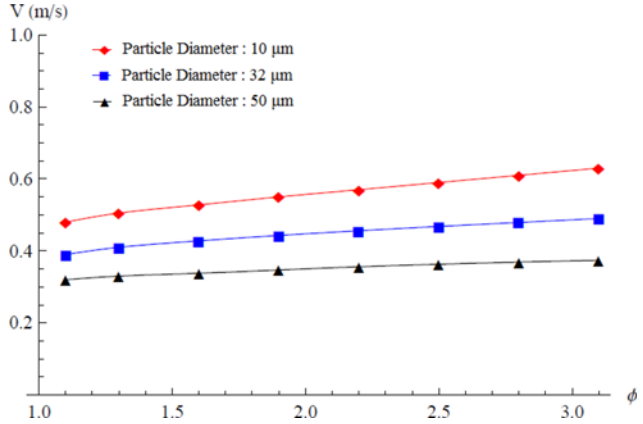

Fig. 6. Flame speed as a function of equivalence ratio in lycopodium particles for different particle diameters.

CONCLUSIONS

In the mathematical model of lycopodium dust cloud combustion presented in this article, a new equation for flame speed and gas temperature distribution in the channel is obtained by solving the two-dimensional energy equations. This equation determines the relationship between flame speed, particle diameter and dust concentration. The partial differential equations have been solved using the separation of variables method in the fuel-lean mixture condition. As shown in the presented figures, flame speed increases with the increase of dust concentration in the lean conditions. In a specific concentration, with the decrease of particle diameter, flame speed increases. Also as expected, flame speed increases gradually with the increase in equivalence ratio. As perceived, the burning velocity profile is boosted by reduction in the particle diameter. In comparison with the one-dimensional condition, the two-dimensional results are closer to the experimental results, and flame speed and flame temperature are in agreement with the experimental results.

NOMENCLATURE

A : parameter characterizing rate of vaporization of fuel particles, Eq. (9)
B : mass fraction of fuel
b′ : heat loss coefficient of gas
C : the specific heat capacity [J/kg°K]
d : diameter of the channel [m]
k : parameter defined in Eq. (9)
n_s : number of particles per unit volume
Q : heat release per unit mass of fuel [J/kg]
Q_v : heat associated with vaporizing unit mass of fuel [J/kg]
r : radius of particle [m]
R : parameter defined in Eq. (9)
S : parameter defined in Eq. (9)
T : temperature [°K]
V : velocity [m/s]
w_f : heat release rate of fuel [kg/m^{3}s]
w_v : heat associated with vaporizing rate of fuel [kg/m^{3}s]

Greek Symbols

β : parameter defined in Eq. (20)
γ : parameter defined in Eq. (20)
δ : flame zone thickness [m]
θ : parameter defined for temperature
θ_s : parameter defined for solid phase temperature in Eq. (23)
θ_{si} : parameter defined for solid phase ignition temperature in Eq. (26)
λ : thermal conductivity of gas [W/m°K]
ξ : parameter defined in Eq. (23)
ρ : density [kg/m^3]
φ : equivalence ratio

Subscripts

g : gas

f : flame
v : vaporization
u : unburned
s : particle
si : particle at the beginnings of burning
st : stoichiometric condition

REFERENCES

1. J. L. Krazinski, R. O. Buckius and H. Krier, *Prog. Energy Combust. Sci.*, **5**, 31 (1979).
2. M. Hertzberg, K. L. Cashdollar and I. A. Zlochower, *Symp. (Int.) Combust.*, **21**, 303 (1988).
3. A. L. Berlad, H. Ross, L. Facca and V. Tangirala, *Combust. Flame*, **82**, 449 (1990).
4. J. H. Sun, R. Dobashi and T. Hirano, *Symp. (Int.) Combust.*, **27**, 2405 (1998).
5. C. Proust, *Experimental determination of the maximum flame temperatures and of the laminar burning velocities for some combustible dust-air mixtures*, Proceedings of the Fifth International Colloquium on Dust Explosions, Pultusk, Poland (1993).
6. Y. Shoshin and E. Dreizin, *Combust. Flame*, **133**, 275 (2003).
7. Z. Chen and B. Fan, *J. Loss Prev. Process Ind.*, **18**, 13 (2005).
8. S. Goroshin, M. Kolbe and J. H. S. Lee, *Symp. (Int.) Combust.*, **28**, 2811 (2000).
9. O. S. Han, M. Yashima, T. Matsuda, H. Matsui, A. Miyake and T. Ogawa, *J. Loss Prev. Process Ind.*, **13**, 449 (2000).
10. O. S. Han, M. Yashima, T. Matsuda, H. Matsui, A. Miyake and T. Ogawa, *J. Loss Prev. Process Ind.*, **14**, 153 (2001).
11. C. Proust, *J. Loss Prev. Process Ind.*, **19**, 89 (2006).
12. C. Proust, *J. Loss Prev. Process Ind.*, **19**, 104 (2006).
13. M. Bidabadi and A. Rahbari, *Combust., Explos. Shock Waves*, **45**, 278 (2009).
14. M. Bidabadi and A. Rahbari, *J. Mech. Sci. Technol.*, **23**, 2417 (2009).
15. M. Bidabadi, A. Haghiri and A. Rahbari, *Int. J. Therm. Sci.*, **49**, 534 (2010).
16. M. Bidabadi, A. Shakibi and A. Rahbari, *J. Taiwan Inst. Chem. Eng.*, **42**, 180 (2011).
17. M. Bidabadi, A. H. Ameri Natanzi and S. A. Mostafavi, *Powder Technol.*, **217**, 69 (2012).
18. W. Gao, T. Mogi, J. Sun, J. Yu and R. Dobashi, *Powder Technol.*, **249**, 168 (2013).
19. M. Jadidi, M. Bidabadi and M. E. Hosseini, *Proc. Inst. Mech. Eng., Part G*, **223**, 915 (2009).
20. S. Goroshin, M. Bidabadi and J. H. S. Lee, *Combust. Flame*, **105**, 147 (1996).